Journal Pre-proofs

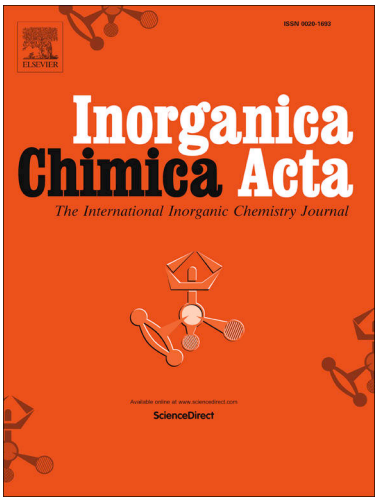

Research paper

A highly sensitive and selective chemosensors for detection of Zn^{2+} and its application in live cell imaging

Yang Hu, LongChao Du, Jie Yang

PII: S0020-1693(20)30403-5
DOI: https://doi.org/10.1016/j.ica.2020.119675
Reference: ICA 119675

To appear in: *Inorganica Chimica Acta*

Received Date: 29 February 2020
Revised Date: 12 April 2020
Accepted Date: 13 April 2020

Please cite this article as: Y. Hu, L. Du, J. Yang, A highly sensitive and selective chemosensors for detection of Zn^{2+} and its application in live cell imaging, *Inorganica Chimica Acta* (2020), doi: https://doi.org/10.1016/j.ica.2020.119675

A highly sensitive and selective chemosensors for detection of Zn^{2+} and its application in live cell imaging

Yang Hu, LongChao Du*, Jie Yang

School of Chemistry and Chemical Engineering & the Key Laboratory of Environment-friendly Polymer Materials of Anhui Province, Anhui University, Hefei, PRC

A novel salen derivative, named as 6,6'-((1E,1'E)-(1,2-phenylenebis(azaneylylidene))bis(methaneylylidene))bis(4-(4-iodobutyl)-2-methylphenol) (PA), was obtained for the detection of Zn^{2+}. PA exhibited highly sensitive and selective via a chelation mechanism, which was promoted by Zn^{2+}, accompanied by enhanced fluorescence. After adding various metal ions in the PA solution, only Zn^{2+} caused PA fluorescence enhancement. Other cations (such as Ag^{+}, Al^{3+}, Ba^{2+}, Ca^{2+}, Cd^{2+}, Cr^{3+}, Cu^{2+}, Fe^{3+}, Hg^{2+}, K^{+}, La^{3+}, Li^{+}, Mg^{2+}, Na^{+}, Ni^{2+} and Pb^{2+}) cannot induce similar response. The binding stoichiometry and detection limit was 1:1 and 16.3 nM, respectively, which is superior to the reported Zn^{2+} fluorescent probes based on salen derivatives. The binding process was reasonably speculated by fluorescence measurements, infrared spectroscopy, ^{1}H-NMR titrations, FT-IR, mass spectroscopy (MS) and density functional theory (DFT) calculation. In addition, PA can be used for Zn^{2+} fluorescence imaging in HeLa cells. This work indicated that this probe would be of great application prospect in medical diagnosis.

Keywords: Fluorescence enhancement; Salen base; Zinc ion; Cell imaging

1. INTRODUCTION

School of Chemistry and Chemical Engineering & the Key Laboratory of Environment-friendly Polymer Materials of Anhui Province, Anhui University, Hefei, PRC
E-mail: dulongchao@sina.com

Metal ions are widely present in tissue cells and body fluids, affecting human physiological and pathological health all the time.[1, 2] In general, proper levels of metal ions can effectively maintain biological processes. Once the ion is excessive or missing, it will cause homeostasis imbalance, leading to a series of serious diseases.[3-5] Among metal ions, zinc ions are abundantly present in living organisms due to the existence of various coordination characteristics.[6] The content of zinc in the human body is second only to iron, and it is the second most transition metal element. It is widely present in human cells and plays an important role in cell metabolism, gene expression, body immunity, and nerve transmission.[7-11] Although the metal proteins of Zn^{2+} ions are tightly bound, a few Zn^{2+} are still free in the cell. 5-20% of Zn^{2+} is accumulated in presynaptic cells in the brain, and many free Zn^{2+} are also found in cells of the hippocampus.[12] Zn^{2+} controls the excitability of the brain and displays a pivotal role in synaptic plasticity.[13] Meanwhile, Changes in zinc concentration often indicate the occurrence of certain diseases. For example, too high or too low zinc concentration may lead to physiological disorders such as enzyme activity disorders, gene expression errors, apoptosis, and blocked neurotransmission.[14, 15] Therefore, designing a chemical sensor that can sensitively and efficiently detect Zn^{2+} is a very crucial subject in the field of neurobiology.[16, 17]

Because they show a pivotal role in diverse biological systems, the detection of metal ions is particularly important in the fields of biomedicine and analysis.[18-21] Over the past few decades, several analytical tools have been used to analyze Zn^{2+}, such as ICP-AES, AAS, and instrumental neutron activation analysis.[22-25] However, the cost of the instrument is high and sample preparation is cumbersome.[26] The fluorescent probe technology, which has the advantages of low cost, fast response time, simple operation, and low detection limit, has become a research method for

quantitative and qualitative analysis of ions and molecules in biological cells. More importantly, Zn^{2+} can be detected while maintaining cell viability. These advantages have prompted researchers to develop new chemical sensors and apply them to the fields of chemistry, biochemistry, and cell imaging.[27-32] Therefore, chemical sensors such as acetaminoquinoline[33], iminocoumarin[34] and tetrazole[35] have been developed to detect Zn2+ ions. However, research on Salen-based chemical sensors has not received sufficient attention. Salen ligands have excellent photophysical properties. Moreover, these salen ligand not only comprises N2O2 coordination pocket, which can easily accommodate various metal ions, but also can easily introduce various substituents into the aromatic ring to adjust the selectivity and sensitivity of the fluorescent chemical sensor.

Here, we designed a novel Salen-based zinc ion sensor PA (Scheme 1). Compound PA could detect Zn^{2+} by a significant fluorescence enhancement and their biological imaging in Hela cells was studied. They were expected to be applied to the qualitative analysis and quantitative detection of metal ions in the environment or in biomedicine.

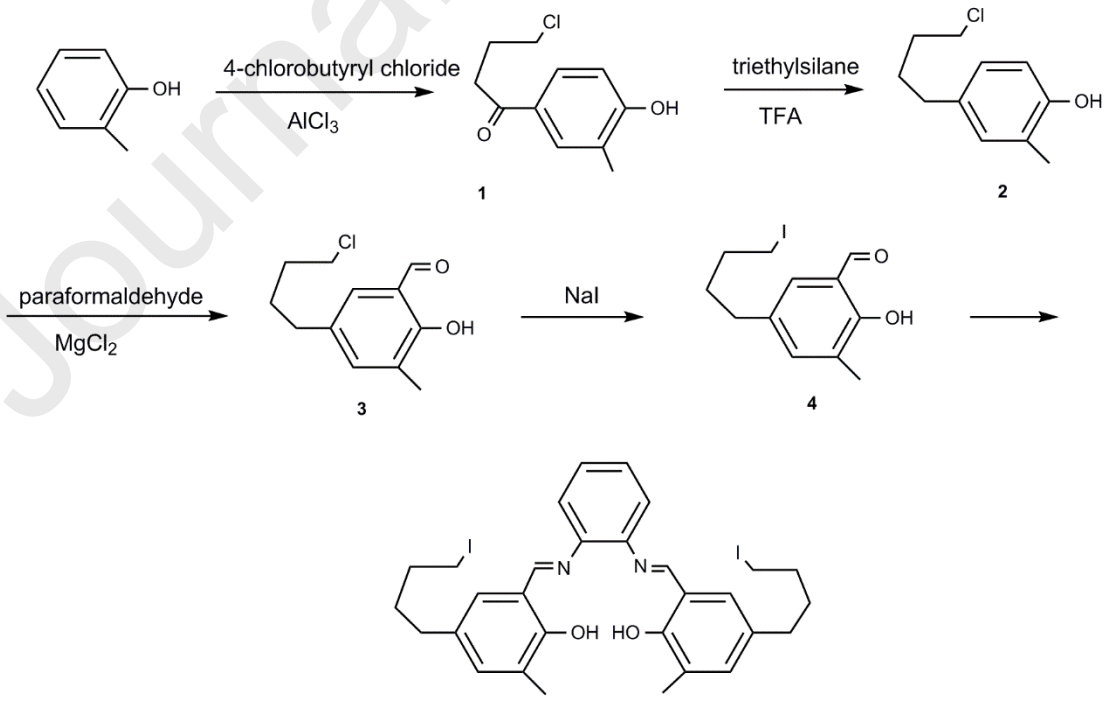

Scheme 1. Synthsis of PA.

2. EXPERIMENTAL

2.1. Materials and instrumentation

Reactions were carried out under inert atmosphere in Schlenk glassware or in a purified nitrogen-filled drybox. Except ethanol was distilled using sodium, solvents (THF, CH_2Cl_2, CH_3CN,) were dried using a purification system composed of calcium hydride. N, N-dimethylformamide (DMF) was HPLC grade and had no fluorescent impurities. The solutions of various metal ions were prepared from nitrate salts. Deionized water was used in the experiment. General chemical reagent were purchased from Shanghai Macklin Biochemical Co, Aladdin Industrial Co, or Shanghai Richjoint Chemical Reagents Co., and used with as received.

The samples were made into KBr tablets, and the Fourier transform infrared (FTIR) spectra were collected on a Vertex80. ^{1}H-NMR spectra were recorded on a NMR spectrometer (AVANCEII, 400MHz) at room temperature. Samples were dissolved in $CDCl_3$ or CD_3SOCD_3 with tetramethylsilane as an internal standard. All spectral characterizations were performed in HPLC-grade solvents in a 10 mm quartz cell at a constant temperature of 20°C. UV-vis spectra were carried out in a Shimadzu UV-3600 spectrophotometer. The fluorescence emission spectra were obtained on a Perkin Elmer LS-55 FL spectrophotometer. The mass spectra were obtained on a Bruker Autoflex III time of flight mass spectrometer.

2.2. Synthesis

The synthetic route to PA was illustrated in Scheme 1. Compound 1-4 were prepared according to literatures reported previously.[36] Detailed synthetic procedures were described below.

Synthesis of PA: Compound 4 (1.04g, 3.27mmol) was dissolved in the ethanol in a three-neck round flask under a N_2 atmosphere. The reaction mixture was stirred at 80℃ for 8 hours. After completion of reaction, the solution was placed in the ice bath for 2h. The product was a yellow solid 0.43g 43%). IR (KBr) (Fig. S5): 3180cm^{-1}(Ar-OH), 1618cm^{-1}(C=N). ^{1}H-NMR (400MHz, DMSO) (Fig. S6): δ=13.07(s, 2H, Ar-OH), 8.86 (s, 2H, C=N), 7.48-7.37(m, 4H, Ar-H), 7.29(s, 2H, Ar-H), 7.17(s, 2H, Ar-H), 3.29-3.25(m, 4H, CH_2I), 2.58(m, 4H, Ar-CH_2), 2.17(s, 6H, Ar-CH_3), 1.85-1.57 (m, 8H, CH_2CH_2). ^{13}C-NMR (400MHz, $CDCl_3$) (Fig. S7): 164.41, 156.01, 144.17, 136.10, 131.46, 127.99, 126.56, 121.92, 121.05, 117.03, 34.99, 32.10, 29.22, 15.34, 6.96. ESI-MS m/z (Fig. S8): $[PA+H]^+$, 709.87.

2.3. Preparation of working solutions and determination of UV–Vis and fluorescence spectroscopy

The sensor PA (3.54 mg, 5.0×10^{-3} mmol) was dissolved in 5mL of DMF to prepare a 1.0×10^{-3} mol/L stock solution. Take 1 mL from the stock solution and add to a 100 mL volumetric flask. Use a pipette to take 1 mL of the stock solution into a 100 mL volumetric flask and prepare a measurement solution with a final concentration of 1×10^{-5} mol/L. The stock solutions (1.0×10^{-3} mol/L) of various metal ions (Ag^+, Al^{3+}, Ba^{2+}, Ca^{2+}, Cd^{2+}, Cr^{3+}, Cu^{2+}, Fe^{3+}, Hg^{2+}, K^+, La^{3+}, Li^+, Mg^{2+}, Na^+, Ni^{2+}, Pb^{2+} and Zn^{2+}) were prepared in deionized water with corresponding nitrates. In the spectrum measurement experiment, 3 mL (1×10^{-5} mol/L) of the working solution was added to a quartz optical

cell with an optical path of 1cm, and then an equal amount of a metal ion solution (3 μL) was added. The fluorescence spectra of the samples were recorded at an excitation wavelength of 328 nm. Both the excitation and emission slit widths were 20nm.

3. RESULTS AND DISSCUSSION

3.1. Synthesis

The synthesis of salen bases probe (PA) is shown in Scheme 1. First, using Al_2O_3 as a catalyst, N_2 was introduced under low temperature conditions, and acylation of o-cresol and 4-chlorobutyryl chloride occurs in CH_2Cl_2 to form compound 1 (Fig. S1). Subsequently, compound 1 and triethylsilane reacted in trifluoroacetic acid at room temperature. Si-H bond breaks, and H attacks C=O in compound 1 to form compound 2 (Fig. S2). In the next step, compound 2 was introduced into the aldehyde group by using acetonitrile as a solvent and reacting with paraformaldehyde and triethylamine under a N_2 atmosphere to obtain compound 3 (Fig. S3). The chloro group of compound 3 was substituted with I^- in a refluxing solvent of CH_3CN to get compound 4 (Fig. S4). The condensation reaction of compound 4 with amine compounds was a crucial step to synthesize the desired product. The intermediates compound 1-4 and final product PA were characterized with ^{1}H-NMR, FT-IR and ESI-MS spectra. The formation of PA was confirmed by the appearance of a characteristic N=CH band at about 1618 cm^{-1} in its FTIR spectrum. The ^{1}H-NMR spectrum of PA exhibited imino proton (-CH=N-) at 8.86 ppm, which confirmed the formation of PA.

3.2. Spectral studies

The selectivity to various metal cation of PA was investigated by UV-vis and

fluorescence spectroscopy. As shown in Figure S9, absorption spectra were measured upon addition of various metal cations (Ag^{+}, Al^{3+}, Ba^{2+}, Ca^{2+}, Cd^{2+}, Cr^{3+}, Cu^{2+}, Fe^{3+}, Hg^{2+}, K^{+}, La^{3+}, Li^{+}, Mg^{2+}, Na^{+}, Ni^{2+}, Pb^{2+} and Zn^{2+}). PA shows weaker absorption peaks at 278nm and 328nm. It can be attributed to the intermolecular charge transfer (ICT) of long conjugated molecules and the C=N group issued transition of π-π*, respectively. Upon the addition of Zn^{2+} to the solution of PA(10μmol), the absorption spectrum of the mixed solution changed greatly, and the maximum absorption wavelength was red-shifted from 328nm to 419nm. The cause of this phenomenon may occur on the ligand-to-metal charge transfer (LMCT) between PA and Zn^{2+} ions. The fluorescence spectrum of PA (10.0 μM) and PA upon addition of various metal ions were recorded at the excitation wavelength of 328 nm in DMF. As shown in Figure 1, the addition of Zn^{2+} greatly stimulated the fluorescence of PA, and the fluorescence intensity was increased 14 times compared to the original. Accompanying the blue shift phenomenon, the emission peak shifted from 484 nm to 440 nm. At the same time, this phenomenon was detected with the naked eye under a 365 nm UV lamp. We assumed that a fluorescent complex was formed between PA and Zn^{2+}. Since the complex PA+Zn^{2+} could inhibit both the photoinduced electron transfer (PET) processes and the C=N isomerization (rotation) process in the salen structure, the fluorescence of the system was enhanced significantly. Under identical conditions, no obvious response could be observed upon the addition of other ions including Ag^{+}, Al^{3+}, Ba^{2+}, Ca^{2+}, Cd^{2+}, Cr^{3+}, Cu^{2+}, Fe^{3+}, Hg^{2+}, K^{+}, La^{3+}, Li^{+}, Mg^{2+}, Na^{+}, Ni^{2+} and Pb^{2+}. It was hinted that PA can be used as a fluorescence sensor with good selectivity for Zn^{2+}.

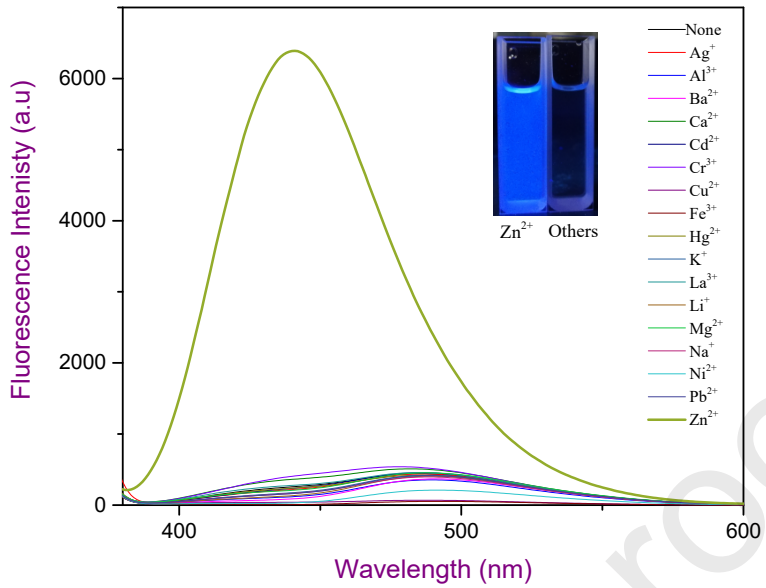

Figure 1. Fluorescence responses of PA (10 μM) in DMF upon the addition of 1.0 equiv various metal ions (λ_{ex}=328nm); The insert shows the fluorescence color of PA with Zn^{2+} and other metal ions under 365 nm UV lamp.

In order to understand the sensing process and binding form of PA to Zn^{2+}, fluorescence titration were conducted that a gradually increasing amounts of Zn^{2+} was added to a solution of PA in DMF, and a significant fluorescence enhancement was observed. As shown in Figure 2, during the titration of Zn^{2+} with PA, a new emission band was formed at 440 nm. This was because the addition of Zn^{2+} inhibited the occurrence of the PET process of PA and C=N isomerization. When Zn^{2+} was added to 1 equivalent, it could be observed that the fluorescence emission intensity reaches a maximum. The absolute quantum yield of PA was 0.03 and PA+Zn^{2+} was 0.48 in DMF. To support the binding stoichiometry of PA+Zn^{2+} complex, Job plot method was performed. From the results shown in Figure 3, it could be seen that the highest point appeared at mole fraction of 0.50 for Zn^{2+}. The results had indicated that the binding modes of PA+Zn^{2+} was stoichiometry of 1: 1.

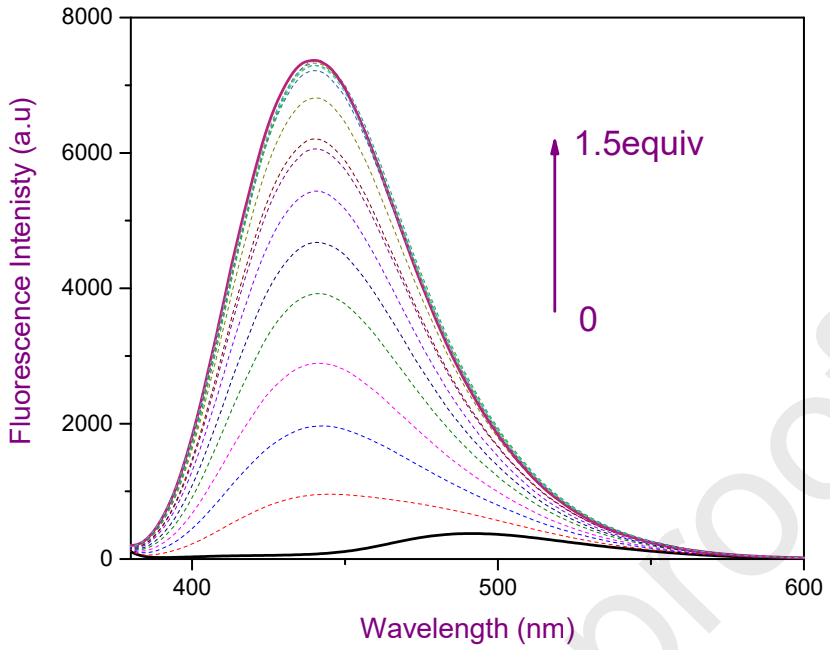

Figure 2. Fluorescence titration of PA (10μM) upon the addition of Zn^{2+} (0-1.5equiv) in DMF (λ_{ex}=328nm).

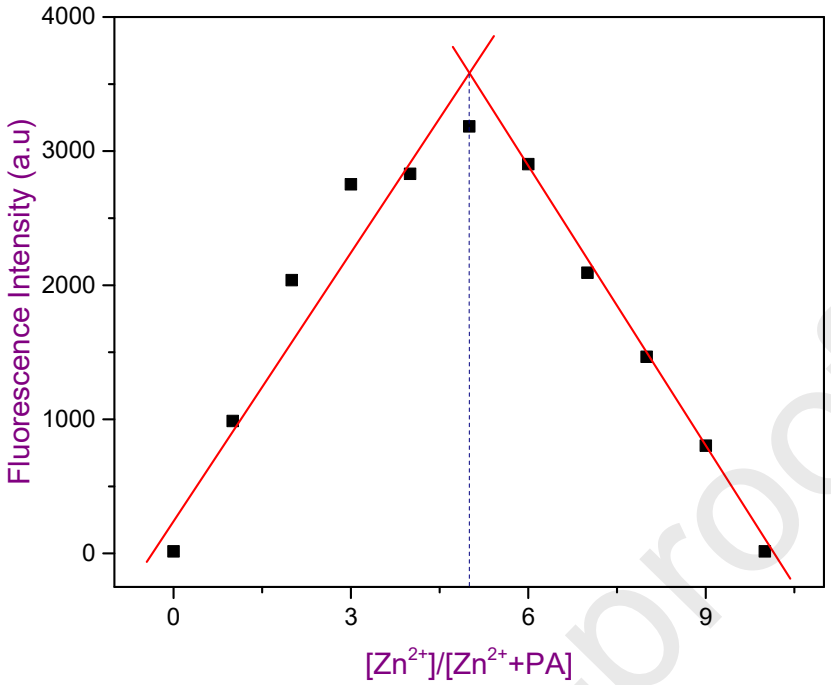

Figure 3. Job's plots for PA and Zn^{2+}. The total concentration PA and Zn^{2+} kept at 10μmol/L with λ_{ex}=360nm.

According to the modified Benesi-Hildebrand equation, the binding constant of PA+Zn^{2+} could be determined from the fluorescence titration curve of the corresponding complex. Fluorescence spectral data was analyzed using the following equation (1):

$$\frac{1}{F - F_0} = \frac{1}{K_a(F_{max} - F_{min})[Zn^{2+}]} + \frac{1}{F_{max} - F_0} \quad (1)$$

K_a was the binding constant of Benesi-Hildebrand equation. F_0, F, and F_{max} were the emission intensities at 440 nm of PA, at tested zinc concentration, and at a concentration of complete interaction, respectively. As shown in Figure 4a, there was an excellent linear relationship between $1/(F-F_0)$ and the reciprocal of the concentration of Zn^{2+} (R^2=0.9904) in the range of 0 to 1.4 equivalents of Zn^{2+} ion concentration. The association constant (K_a) was 2.94×10^4 M^{-1}.

The limit of detection (LOD) was also calculated based on fluorescence titration. First, the emission intensity of PA in DMF (10 μM) needed to be measured separately 10 times to obtain the standard deviation of the blank measurement. Second, 0-42 μM Zn^{2+} was added to the PA (10 μM) solution, and a good linear relationship was found between the fluorescence intensity at 440 nm and the Zn^{2+} concentration between 0 and 42 μM. Finally, the detection limit was calculated according to the following formula: detection limit=3σ/K, where K was the slope of the fluorescence intensity and the Zn^{2+} concentration, and σ was the standard deviation of the blank measurement. As shown in Figure 4b, the detection limit was determined as 1.635×10^{-8} M pointing to the high detection sensitivity. Compared with the previously reported values of Zn^{2+}-fluorescence sensors, the LOD of PA presented here was lower.[37, 38]

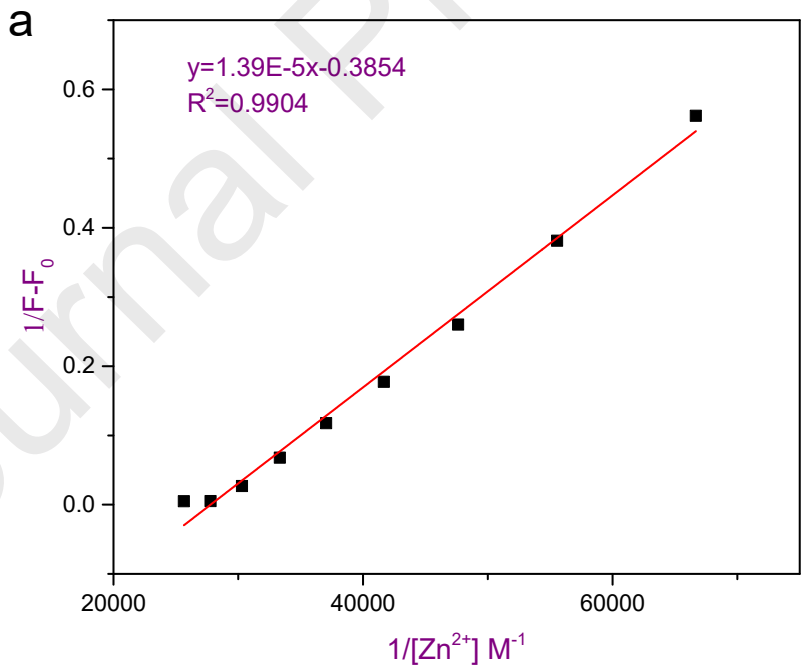

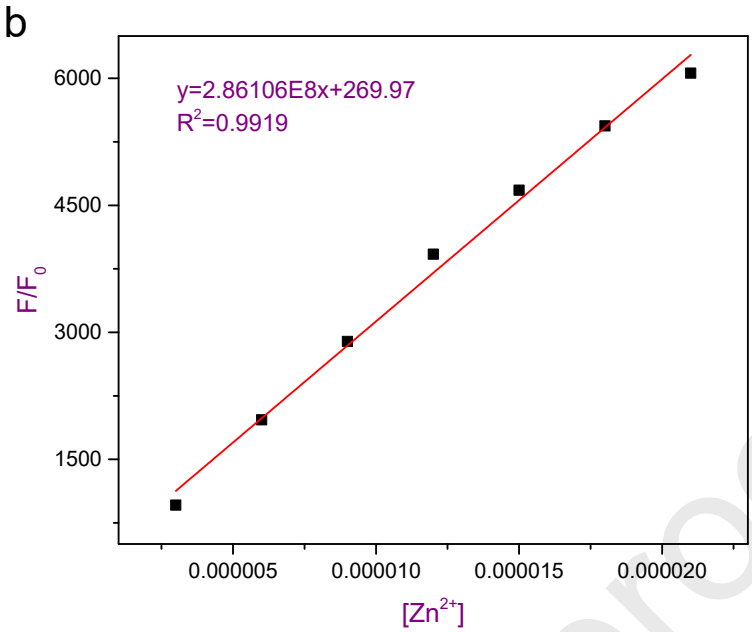

Figure 4. (a) A certain linear relationship between reciprocal of fluorescence intensity [1/F-F_0] and reciprocal of concentration of Zn^{2+} solution (λ_{ex}=328nm); (b) A linear relationship between F/F_0 and $[Zn^{2+}]$.

High selectivity was also a valid criterion for the success of the probe design. In order to evaluate the affinity of the probes for different metal ions, the competition experiments of PA (10 μM) were performed with various metal ions (10 μM) in DMF solution. The corresponding fluorescence intensity was shown in Figure 5. Obviously, in addition to the slight fluorescence change caused by Cu^{2+} and Fe^{3+}, Zn^{2+} can cause significant fluorescence enhancement in different metal ion solutions. When other common metal ions are present, such as Ag^{+}, Al^{3+}, Ba^{2+}, Ca^{2+}, Cd^{2+}, Cr^{3+}, Hg^{2+}, K^{+}, La^{3+}, Li^{+}, Mg^{2+}, Na^{+}, Ni^{2+}, and Pb^{2+}, they did not interfere with the detection of Zn^{2+}. These results indicated that PA can be used for the selective and sensitive detection of Zn^{2+} in DMF.

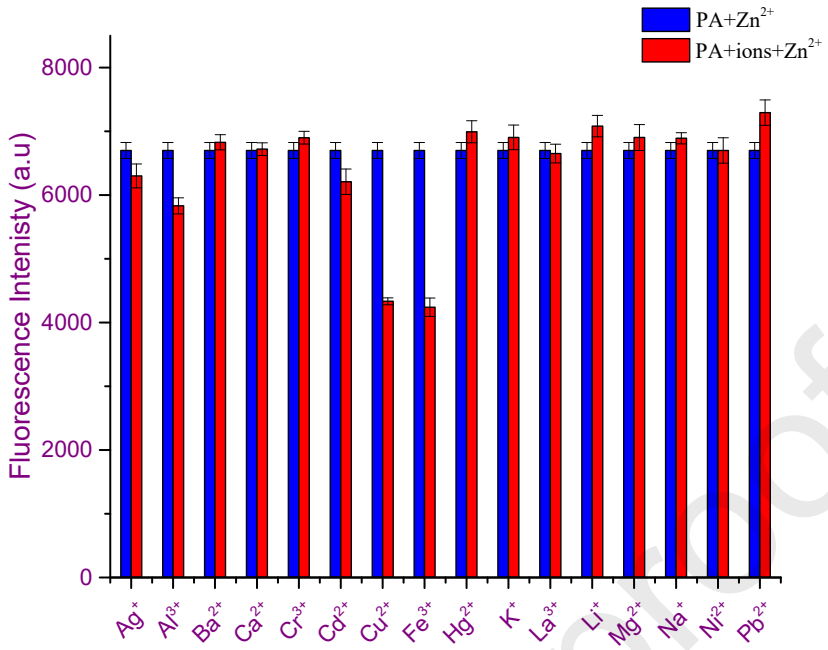

Figure 5. Fluorescence spectra of PA (10μM) containing Zn^{2+} (1.0equiv) and other competitive metal ions (1.0equiv) in DMF solution.

3.3 Binding mechanism of PA to Zn^{2+}

To confirm the complexation mechanism between PA and Zn^{2+} ions, ^{1}H-NMR of PA in the absence and presence of Zn^{2+} was measured using a NMR spectrometer. As shown in Figure 6, the chemical shifts at 13.07 and 8.86 ppm may be assigned to the phenolic hydroxyl group and N=CH band of the probe PA, respectively. Once Zn^{2+} was added, the phenolic hydroxyl groups of the probe PA completely disappeared at δ13.07, indicating that Zn^{2+} and the phenolic hydroxyl groups of the probe PA may have been combined. In addition, the combination of Zn^{2+} changed the chemical shift of N=CH band. Compared with the free probe, the peak of N=CH band in PA+Zn^{2+} had moved from the position of δ 8.86 to the position of δ 9.85, indicating that Zn^{2+} may react with N=CH band. Similarly, FT-IR studies clearly show that the phenolic hydroxyl bands of PA appearing at 3180 cm^{-1} in the presence of Zn^{2+} ions disappear. At the same time, the

C-O band at 1648 cm^{-1} was significantly enhanced in the FT-IR spectrum (Figure S10). Formation of PA+Zn^{2+} was also evidenced by ESI-mass test. The MS spectrum of the PA+Zn^{2+} complex in DMF solution was shown in Figure S11. The MS spectrum exhibited that the peak of m/z: 772.43 was suggestive to $[PA+Zn^{2+}+H^{+}]^{+}$. These results supported the coordination of phenol-OH and imine nitrogen with Zn^{2+} in PA after adding Zn^{2+}. Based on the analysis of ^{1}H-NMR, FT-IR, ESI-mass test and Job plot, the 1:1 binding of PA with Zn^{2+} was suggested, as displayed in Scheme 2.

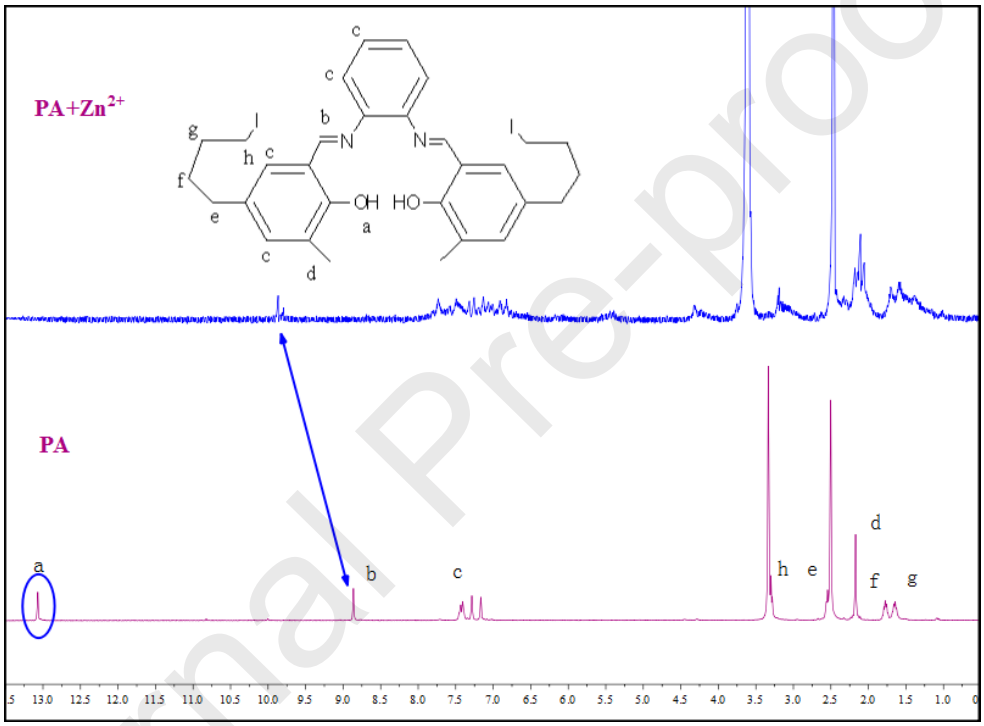

Figure 6. ^{1}H-NMR titration spectral of PA upon addition of Zn^{2+} in CD_3SOCD_3-D_2O (v/v=1:1).

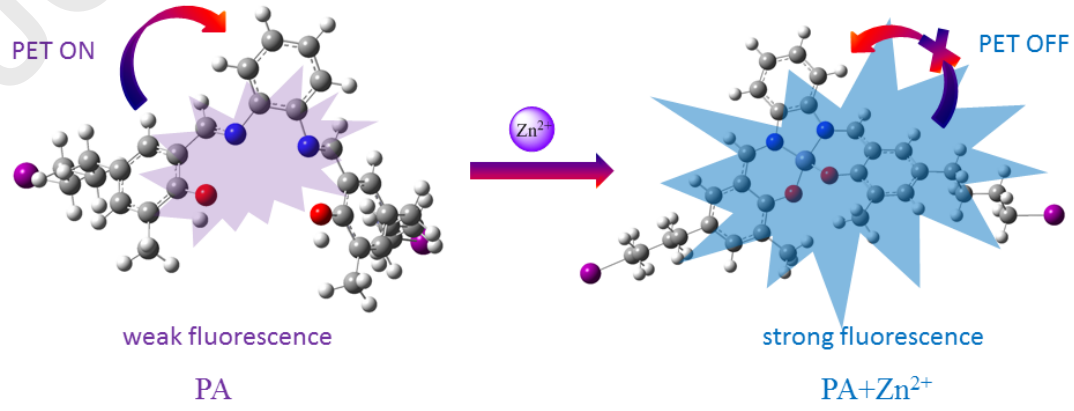

Scheme 2. The proposed binding mode of Zn^{2+} with PA.

In order to understand the possible mechanism of the interaction between PA and Zn^{2+} from a theoretical perspective, the geometric structure of the probe PA and PA+Zn^{2+} was optimized by density functional theory (DFT) based on the previously estimated binding model. The Gaussian 09 program was used to obtain the singlet excited states of the probe PA and PA+Zn^{2+} at the B3LYP/6-31G level. From the calculation results (Figure 7), The energy gap between the LUMO and HOMO levels in the probe PA was 3.99 eV, while the energy gap between the LUMO and HOMO levels in PA+Zn^{2+} was 3.74 eV. It could be found that the band gap energy (3.74 eV) between HOMO and LUMO of PA+Zn^{2+} was lower than the band gap energy (3.99 eV) of the probe PA, which indicated that the probe PA formed a more stable complex after combining with Zn^{2+}. As shown in the Figure 7, the LUMO electron density of the probe PA was mainly distributed in the phenolic hydroxy-benzene moiety. The HOMO electron density of the phenolic hydroxy-benzene moiety of the probe PA decreased relative to the LUMO electron density, and the HOMO electron density of the o-phenylenediamine moiety increased. These results indicated that the PET pathway of the phenolic hydroxy-benzene moiety to the o-phenylenediamine moiety of the probe PA was open. Once PA was coordinated with Zn^{2+}, the LUMO and HOMO electron density of PA+Zn^{2+} were evenly distributed in the phenolic hydroxy-benzene moiety and o-phenylenediamine moiety. And after PA coordinated with Zn^{2+}, the LUMO and HOMO electron density decreased. These results indicated that the PET pathway of the phenolic hydroxy-benzene moiety to the o-phenylenediamine moiety of the probe PA was blocked. As the previous experimental results was shown, PA and PA+Zn^{2+} had similar band gap energies between LUMO and HOMO, suggesting their similar absorption peaks. Not surprisingly, the experimental results were confirmed by the

conclusions of theoretical calculations.

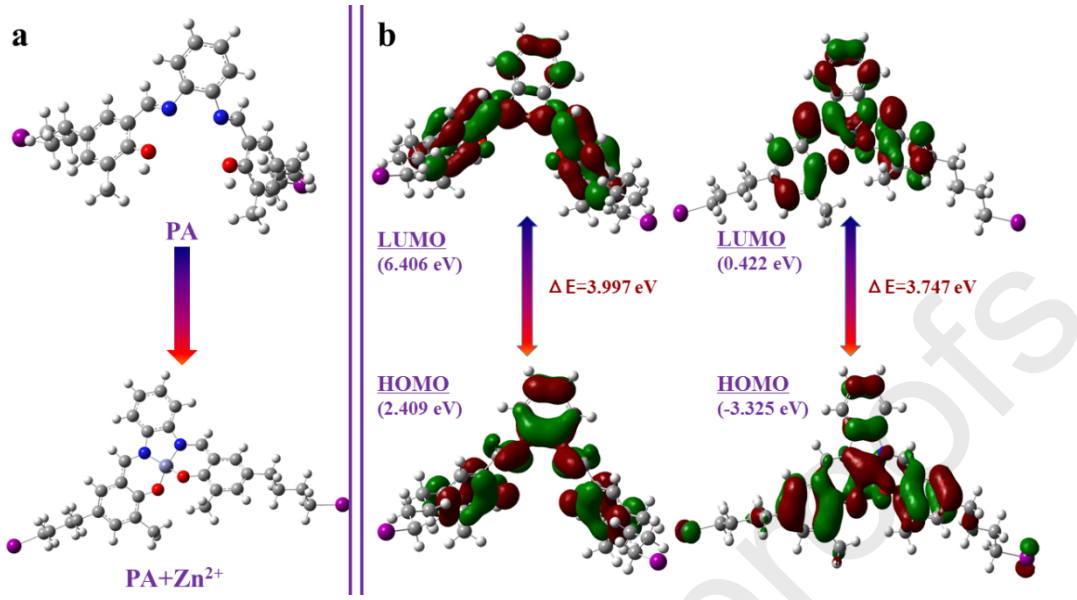

Figure 7. (a) Optimized structures of PA and PA+Zn^{2+}; (b) HOMO/LUMO energy levels and the contour diagrams of PA and PA+Zn^{2+} by DFT calculation.

3.4 Cyclic Voltammetry Experiments

Cyclic voltammetry (CV) was used to conduct electrochemical studies to further understand the sensing behavior of PA and Zn^{2+} ions. Initially, a 0.1M TBAP (tetrabutylammonium perchlorate)/CH_3CN solution was used as the electrolyte, and the scanning rate of 0.1 V/s was used to study the electrochemical behavior of PA. It can be seen from Figure 8 that the sensor PA had two oxidation peaks (E_{pa1}=0.985V, E_{pa2}=-0.585V) and one reduction peak (E_{pc}=-1.041V) in the potential range of -1.6V to 1.6V. When Zn^{2+} was added to the DMF solution of PA, it caused obvious behavior in the CV curve. It can be seen from the figure that after the interaction between PA and Zn^{2+}, the redox peak current slightly decreased, and a negative shift occurred. Compared with the previous CV curve of PA, a new reduction peak appeared at the position of E_{pc}=-0.718V. At the position of E_{pa2}=-0.585 V, the oxidation peak of PA+Zn^{2+} decreased

significantly. These changes may be due to the formation of a complex between the probe PA and Zn^{2+} through the O atom and the N atom of the C=N group. The CV curve results indicated that PA and Zn^{2+} ions formed a complex, as displayed in Scheme 2

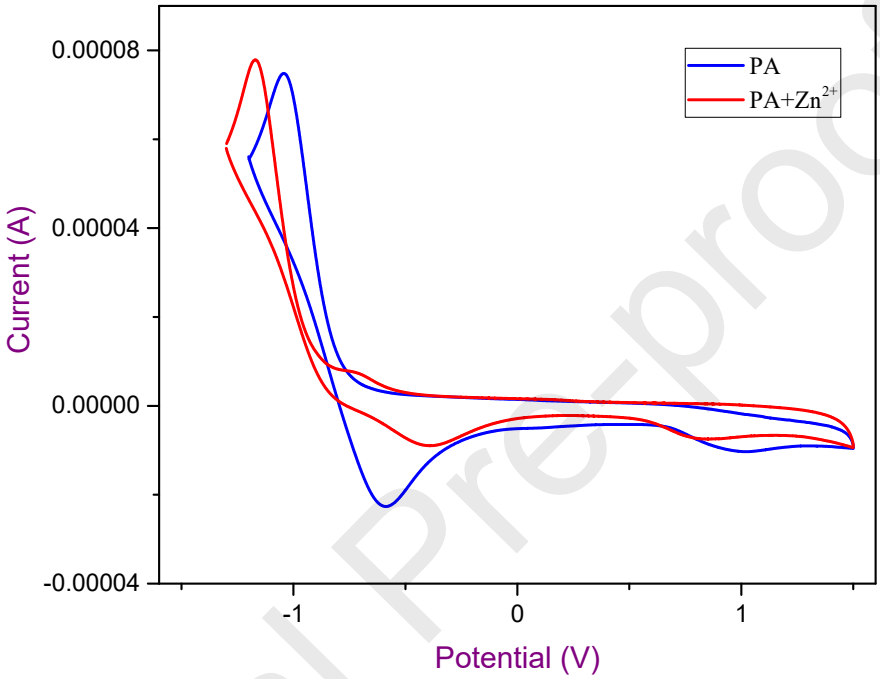

Figure 8. CV profiles of PA and PA+Zn^{2+}.

3.5 In vitro cytotoxicity and imaging Zn^{2+} in Living Cells

Based on the good selectivity and sensitivity of probe PA, the cytotoxicity of probe PA was measured by MTT assay before imaging Zn^{2+} in living cells. HeLa cells were incubated with different concentrations of probe PA (1, 2.5, 5, 10, 15, 20, 25, 30 μM) for 24 hours. As shown in Figure 9, even when the probe PA was at a concentration of 30 μM, the cell viability of HeLa cells was still higher than 80% for an incubation time up to 24 hours. These results indicated that probe PA had low cytotoxicity and good

biocompatibility to live HeLa cells

Subsequently, the practical utility of this probe was explored. In order to explore the application prospects of PA in biological systems, we applied the probe PA to live Hela cells and performed biological imaging experiments to study the sensing performance of the probe PA on Zn^{2+} in the cell matrix. The probe PA was dissolved in DMSO (10^{-3} M) for future use. HeLa cells were incubated with PA solution (10 μM) for 30 minutes, and the change in fluorescence intensity was observed by a confocal fluorescence microscope (Figure 10). As expected, we did not observe fluorescence emission after incubating HeLa cells with probe PA (10 μM) in DMEM for 30 minutes at 37°C. However, in another experimental group, when HeLa cells were pretreated with 10 μL of probe PA (10 μM) for 30 minutes, and then pretreated with Zn^{2+} (10 μM) for 30 minutes, we could detect significant blue fluorescence. The merged image under the bright field image on the fluorescence image shows that the cells pretreated with the probe retained a good morphology, and PA could successfully enter the cells and accumulate in the cytoplasm. This strong fluorescent emission confirmed that the probe was permeable to the cell membrane. These results indicated that probe PA could detect intracellular Zn^{2+} in living cells, and probe PA had good biocompatibility and cell permeability. Therefore, it may be a satisfactory chemical sensor for Zn^{2+} ion imaging in living cells.

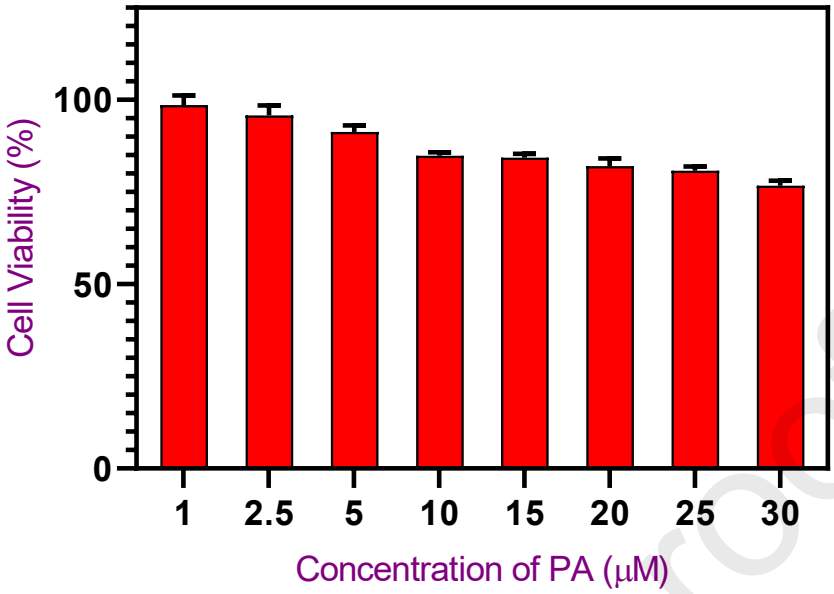

Figure 9. Viability of HeLa cells in the presence of PA as measured by using MTT assay.

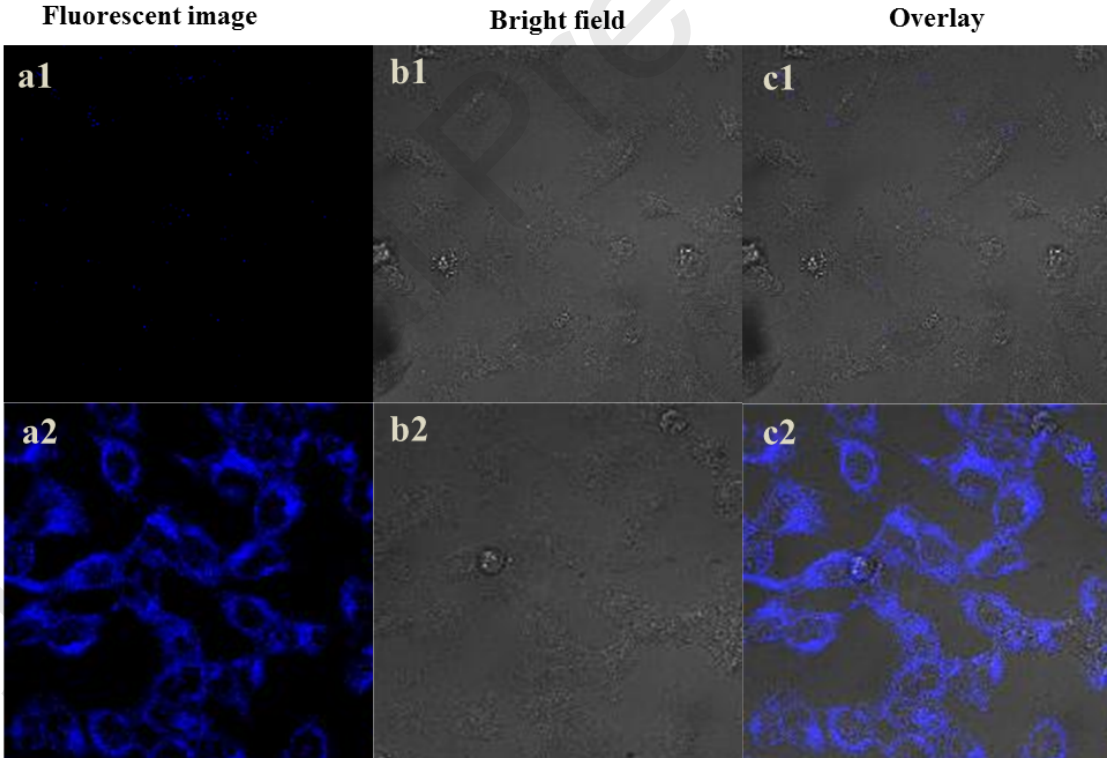

Figure 10. Confocal images of Hela cells: (a1) incubated with PA (10 μM); (a2) further incubated with Zn^{2+} (10 μM); (b1-b2) bright-field images; (c1-c2) merged images.

4. CONCLUSION

In summary, we had successfully prepared a Zn^{2+} fluorescent probe PA with high selectivity and sensitivity. The probe exhibited a remarkable fluorescence enhancement upon addition of Zn^{2+} in DMF solution. The binding stoichiometry and detection limit were 1:1 and 16.3 nM, respectively, which is superior to the reported Zn^{2+} fluorescent probes. The theoretical calculations of Zn^{2+} probe, ^{1}H-NMR, FT-IR, ESI-mass, and cyclic voltammetry tests can agree well with the identification mechanism. In addition, the probe had good biocompatibility and low cytotoxicity, and could be used to detect Zn^{2+} in living HeLa cells.

ACKNOWLEDGEMENTS

The authors are thankful for financial support from the Anhui Provincial Natural Science Foundation (No.1908085MB51), and Anhui Province Key Laboratory of Enviorment-friendly Polymer Materials.

REFERENCES

[1] Z. Xu, K.H. Baek, H.N. Kim, J. Cui, X. Qian, D.R. Spring, I. Shin, J. Yoon, J. Am. Chem. Soc, 132 (2010) 601-610.

[2] Z. Xu, J. Yoon, D.R. Spring, Chem. Soc. Rev, 39 (2010) 1996-2006.

[3] A.K. Boal, A.C. Rosenzweig, Chem. Rev, 109 (2009) 4760-4779.

[4] C. Joseph A, A. Allegra T, R.-T. Karla M, C. Christopher J, Chem. Soc. Rev, 44 (2018) 4400-4414.

[5] T.V. O'Halloran, Science, 261 (1993) 715-725.

[6] A. Ajayaghosh, P. Carol, S. Sreejith, J. Am. Chem. Soc, 127 (2005) 14962-14963.

[7] C.J. Frederickson, J.-Y. Koh, A.I. Bush, Nat. Rev. Neurosci, 6 (2005) 449-462.

[8] E.L. Que, D.W. Domaille, C.J. Chang, Chem. Rev, 108 (2008) 1517-1549.

[9] S. Assaf, S.-H. Chung, Nature, 308 (1984) 734-736.

[10] D.W. Choi, J.Y. Koh, Annu. Rev. Neurosci, 21 (1998) 347-375.

[11] L. Wang, J.-H. Liu, Z.-M. Song, Y.-X. Yang, A. Cao, Y. Liu, H. Wang, Sci. China. Chem, 59 (2016) 910-917.

[12] A. Loas, R.J. Radford, S.J. Lippard, Inorg. Chem, 53 (2014) 6491-6493.

[13] B.K. Bitanihirwe, M.G. Cunningham, Synapse, 63 (2009) 1029-1049.

[14] W. Maret, C. Jacob, B.L. Vallee, E.H. Fischer, P. Natl. A. Sci, 96 (1999) 1936-1940.

[15] M. Shellaiah, Y.-H. Wu, H.-C. Lin, Analyst, 138 (2013) 2931-2942.

[16] J.H. Kim, I.H. Hwang, S.P. Jang, J. Kang, S. Kim, I. Noh, Y. Kim, C. Kim, R.G. Harrison, Dalton. T, 42 (2013) 5500-5507.

[17] N. Narayanaswamy, D. Maity, T. Govindaraju, Supramol. Chem, 23 (2011) 703-709.

[18] P.J. Kraulis, E.A. Merritt, M.E.P. Murphy, C.D. Acta, S. Pecial, S. Ection, L.A. Finney, T.V. O'Halloran, Science, 300 (2003) 931-936.

[19] Q. Lin, Y.Q. Fan, P.P. Mao, L. Liu, T.B. Wei, Chemistry, 24 (2017) 777-783.

[20] Q. Lin, T.-T. Lu, X. Zhu, T.-B. Wei, H. Li, Y.-M. Zhang, Chem. Sci, 7 (2016) 5341-5346.

[21] Y.-M. Zhang, W. Zhu, W.-J. Qu, K.-P. Zhong, X.-P. Chen, H. Yao, T.-B. Wei, Q. Lin, Chem. Commun, 54 (2018) 4549-4552.

[22] A. Rajabi Khorrami, A.R. Fakhari, M. Shamsipur, H. Naeimi, Int. J. Environ. An. Chem, 89 (2009) 319-329.

[23] M. Ghaedi, F. Ahmadi, A. Shokrollahi, J. Hazard. Mater, 142 (2007) 272-278.

[24] K.S. Rao, T. Balaji, T.P. Rao, Y. Babu, G. Naidu, Spectrochim. Acta. B, 57 (2002) 1333-1338.

[25] R. Gulaboski, V. Mirčeski, F. Scholz, Electrochem. Commun, 4 (2002) 277-283.

[26] Q. Lin, X.-M. Jiang, X.-Q. Ma, J. Liu, H. Yao, Y.-M. Zhang, T.-B. Wei, Sensor. Actuat. B. Chem, 272 (2018) 139-145.

[27] Q. Zeng, P. Cai, Z. Li, J. Qin, B.Z. Tang, Chem. Commun, 0 (2008) 1094-1096.

[28] A.P. De Silva, H.N. Gunaratne, T. Gunnlaugsson, A.J. Huxley, C.P. McCoy, J.T. Rademacher, T.E. Rice, Chem. Rev, 97 (1997) 1515-1566.

[29] G.J. Park, J.J. Lee, G.R. You, L. Nguyen, I. Noh, C. Kim, Sensor. Actuat. B. Chem, 223 (2016) 509-519.

[30] L. Tang, Z. Huang, Z. Zheng, K. Zhong, Y. Bian, J. Fluoresc, 26 (2016) 1535-1540.

[31] Q. Lin, K.-P. Zhong, J.-H. Zhu, L. Ding, J.-X. Su, H. Yao, T.-B. Wei, Y.-M. Zhang, Macromolecules, 50 (2017) 7863-7871.

[32] Q. Lin, P.-P. Mao, Y.-Q. Fan, L. Liu, J. Liu, Y.-M. Zhang, H. Yao, T.-B. Wei, Soft Matter, 13 (2017) 7085-7089.

[33] L. Xue, C. Liu, H. Jiang, Org. Lett, 11 (2009) 1655-1658.

[34] K. Komatsu, Y. Urano, H. Kojima, T. Nagano, J. Am. Chem. Soc, 129 (2007) 13447-13454.

[35] K. Ponnuvel, V. Padmini, R. Sribalan, Sensor. Actuat. B. Chem, 222 (2016) 605-611.

[36] S. Sujith, J.K. Min, J.E. Seong, S.J. Na, B.Y. Lee, Angew. Chem, 120 (2008) 7416-7419.

[37] W. Zhu, L. Du, W. Li, J. Zuo, J. Shan, Spectrochim. Acta. A, 203 (2018) 501-509.

[38] L. Du, X. Qin, S. Huang, Int. J. Electrochem. Sci, 13 (2018) 8838-8853.

Author Contribution Statement

LongChao Du: Conceptualization, Methodology, Funding acquisition.

Yang Hu: Investigation, Methodology, Data curation, Software, Writing-Original draft preparation.

Jie Yang: Software.

Graphical Abstract

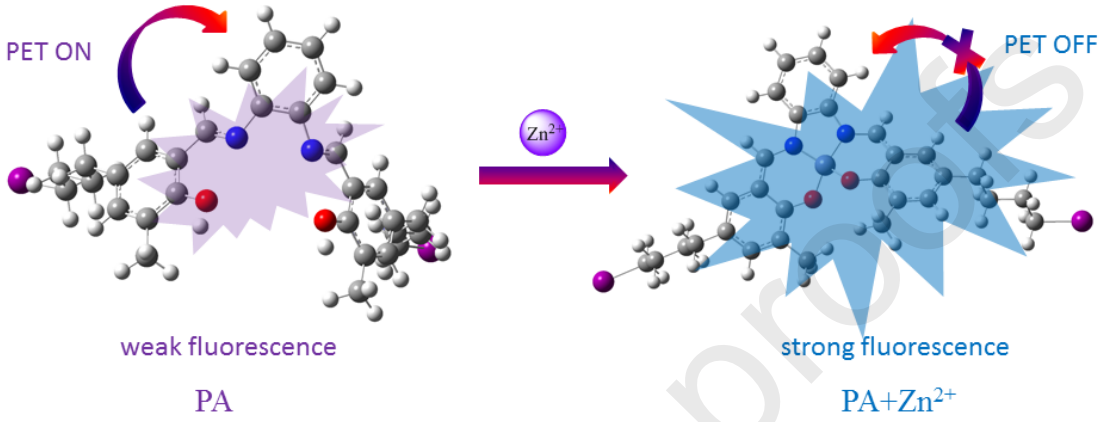

Highlights

- A novel salen derivative was obtained for the detection of Zn^{2+}.
- The probe exhibited a remarkable fluorescence enhancement upon addition of Zn^{2+} in DMF solution.
- The probe had good biocompatibility and low cytotoxicity, and could be used to detect Zn^{2+} in living HeLa cells.